Supplementary Information (SI) for Catalysis Science & Technology.
This journal is © The Royal Society of Chemistry 2024

Catalyst	Light source	Irradiance /(kW m^{-2})	Au diameter /nm	Au loading /wt. %	H_2:CO_2 ratio	Pressure /bar	Additional heating	CO activity	CO selectivity	Reference
Au/TiO_2	Dolan–Jenner broadband visible light source (MI-150)	5.216	3.5	1.4	2:1	10.2	400°C	159.8 mmol g_{cat}^{-1} h^{-1}	>99%	1
	Hg lamp (UV)	1.5	18	0.5	1:1	1	RT	4.144 mmol g_{cat}^{-1} h^{-1}	>99%	2
	Solar simulator (AM 1.5)	14.4	1.6	3.12	1:1	3.5	RT	429 mmol g_{Au}^{-1} h^{-1}	98%	3, 4
	Solar simulator (AM 1.5)	13.9	6	3.9	1:1	3.5	RT	7.81 mmol g_{Au}^{-1} h^{-1}	>88%	5
	Solar simulator (AM 1.5)	13.9	16	3.72	1:1	3.5	RT	0.44 mmol CO g_{Au}^{-1} h^{-1}	>84%	5
Au/Al_2O_3	Dolan–Jenner broadband visible light source (MI-150)	5.216	10	0.7	2:1	10.2	400°C	7.08 mmol g_{cat}^{-1} h^{-1}	>99%	1
	365 nm LED 460 nm LED 5700K white light LED	30.0	2.6	1.7	5:1	1	350°C	1.3 mmol g_{cat}^{-1} h^{-1}	100%	6
	Green LED	2.501	4.3	3.62	4:1	1	330°C	1.06 mmol g_{cat}^{-1} h^{-1}	/	7
	Green LED	2.501	6.7	3.58	4:1	1	330°C	1.18 mmol g_{cat}^{-1} h^{-1}	/	7
	Green LED	2.501	31.3	3.75	4:1	1	330°C	1.36 mmol g_{cat}^{-1} h^{-1}	/	7
Au/SiO_2	Dolan–Jenner broadband visible light source (MI-150)	5.216	2	3.925	2:1	8.1	300°C	11.24 mmol g_{cat}^{-1} h^{-1}	>99%	1, 8
Au/CeO_2	Dolan–Jenner broadband visible light source (MI-150)	5.216	5	3.3	2:1	10.2	400°C	85.02 mmol g_{cat}^{-1} h^{-1}	>99%	1
	Xe Arc lamp	32.0	15	1	4:1	1	RT	7 mmol g_{cat}^{-1} h^{-1}	>99%	9
	Solar simulator (AM 1.5)	8.9	<2	0.41	1:1	3.5	RT	3.9 mmol g_{Au}^{-1} h^{-1}	>98%	This work
	Solar simulator (AM 1.5)	8.9	3.9	1.57	1:1	3.5	RT	1.0 mmol g_{Au}^{-1} h^{-1}	>98%	This work
	Solar simulator (AM 1.5)	8.9	3.8	3.8	1:1	3.5	RT	2.8 mmol g_{Au}^{-1} h^{-1}	>98%	This work
	Solar simulator (AM 1.5)	8.9	3.5	5.8	1:1	3.5	RT	1.8 mmol g_{Au}^{-1} h^{-1}	>98%	This work

Table S1: Literature overview of metal oxide supported Au plasmonic photocatalysts for rWGS.

1 Experimental methods

1.1 Synthesis

CeO_{2-x} particles were synthesised using a hydrothermal method adapted from Zhang et al.[10] The synthesis method was adjusted as to obtain larger (L-HT) and smaller (S-HT) particle sizes. In a typical experiment, $Ce(NO_3)_3 \cdot 6H_2O$ (4.071 g, 9.38 mmol, Thermo Scientific Chemicals, 99.5%) and polyvinylpyrrolidone (PVP) (2.306 g, 20.8 mmol monomer (L-HT); 4.613 g, 41.6 mmol monomer (S-HT), 8,000 average M.W., Acros Chemicals) were dissolved in a 75 ml mixture of ethanol (VWR Chemicals, 96%) and ultra-filtered water (Milli-Q Millipore, Billerica, MA, USA, 18.2 MΩ cm) with a volume ratio of 1:2 and 3:1 for L-HT and S-HT, respectively, in a 100 ml beaker. The mixture was sonicated for two minutes in an ultrasonication bath (Fisherbrand, FB15057) to facilitate PVP dissolution and subsequently stirred with a magnetic stirrer in open air while covered with a watch glass for one hour. Next, the solution was transferred to a Teflon lined autoclave (Parr autoclave, model 4748, 125 ml). The hydrothermal reaction was carried out at 160°C (Binder, ED series 53) for 20h and 14h for L-HT and S-HT, respectively. The autoclaves were left in the oven to cool down. The resulting dispersion was stirred in open air with a magnetic stirrer in a wide, open beaker on a hot plate for 16h at 80°C, and subsequently 2h at 95°C in order to evaporate the solvent. Next, the obtained L-HT and S-HT powders were thermally treated in dry air at 400°C for 2h in an alumina boat crucible, with a heating ramp rate of 3.1°C/min and 0.6 l/min flow, in order to remove organic residues, resulting in large (L) and small (S) CeO_{2-x} powders, respectively. The samples were allowed to cool down inside the tube furnace.

Au nanoparticles were deposited on the CeO_{2-x} support materials by means of a deposition-precipitation method as discussed in our previous work.[5] Urea (0.5 g, 8.33 mmol, VWR Chemicals, 99%) and CeO_{2-x} (500 mg, 2.9 mmol, L or S) were weighed in a 100 ml round bottom flask. Ultra-filtered MilliQ water (50 ml) was added as well as 2.00 ml, 5.18 ml and 8.10 ml of an aqueous solution of $HAuCl_4$ (0.02 M, Alfa Aesar, 99.99%) to obtain catalysts with increasing gold loadings, denoted as 1.5Au/S (1.5 wt. % Au), 4Au/S (4.0 wt. % Au), 4Au/L (4.0 wt. % Au) and 6Au/S (6.0 wt. % Au). The round bottom flask was ultrasonicated in an ultrasonication bath for one minute and next stirred and heated with a heat mantle under reflux for 3h at 80°C. Subsequently, 4.00 ml, 10.36 ml and 16.20 ml of freshly prepared $NaBH_4$ solution (0.1 M, Acros Organics, 99%) was added dropwise under continuous stirring, for 1.5Au/S, 4Au/S, 4Au/L and 6Au/S respectively, and left to stir for 1h at 80°C under reflux. Then, the samples were centrifugated and washed three times with ultra-filtered water and once with ethanol. Finally, the catalysts were allowed to dry overnight in a fume hood.

An alternative deposition- precipitation method was utilised for synthesis of a 0.4 wt. % Au sample in order to achieve a smaller Au NP size, denoted 0.4Au/S.[3, 4, 11, 12] $HAuCl_4 \cdot 3H_2O$ (7.8 mg, 0.020 mmol, Alfa Aesar, 99.99%) was dissolved in ultra-filtered MilliQ water (100 ml) in a 100 ml round bottom flask. NaOH (50% m/m, Sigma-Aldrich, 98%) was diluted to a concentration of 0.02 M and added dropwise under continuous stirring and pH monitoring until a stable pH of 9 was obtained, under ambient conditions. Next, 1g of S CeO_{2-x} was added to the mixture, and subsequently the pH was readjusted to 9 by dropwise addition of NaOH. The dispersion was allowed to stir for 48 hours and subsequently centrifuged and washed three times with ultra-filtered MilliQ water and once with ethanol and dried overnight in a fume hood. Finally, the sample was thermally treated at 200°C in flow rate dry air (0.6 l/min) for 4 hours, with a heating ramp rate of 2°C/min. The sample was allowed to cool down inside the tube furnace.

Catalysts 4Au/L and 4Au/S were thermally oxidized in dry air (0.6 l/min) at 500°C for 2h, with a heating ramp rate of 4.0°C/min, resulting in samples denoted 4Au/L-O and 4Au/S-O. The 4Au/L and A4u/S catalysts were also thermally reduced in forming gas (5% H_2 in N_2; stationary atmosphere) at 500°C for

2h, with a heating ramp rate of 7.9°C/min. Resulting in samples denoted 4Au/L-R and 4Au/S-R. The samples were allowed to cool down inside the tube furnace.

In order to minimise the impact of possible batch to batch variations, samples of repetitive batches were mixed before carrying out subsequent synthesis steps.

1.2 Characterisation

Transmission electron microscopy (TEM) studies of the CeO_{2-x} support particles were carried out on a FEI Tecnai Spirit operated at 120 kV. At least 90 particles were analysed per sample.

TEM studies of Au/CeO_{2-x} catalysts were carried out at 200 kV with a JEOL ARM 200F probe corrected TEM. Particle imaging was performed in high-angle annular dark field scanning TEM (HAADF-STEM) mode. Energy dispersive X-ray spectroscopy (EDX) spectra were recorded using a 100 mm² Centurio SDD detector. EDX mappings were obtained in STEM mode by acquiring full spectra in grids of 256 x 256 pixels for all magnifications. All mappings were obtained by summation of 50-100 frames, each having 0.1 ms acquisition time per pixel per frame. In this way, the material remained unaffected by the impact of the incident electron beam. EDX mappings were used for material identification, particle size analysis was performed on the corresponding HAADF-STEM images at a consistent magnification level. For particle size distributions at least 90 particles were analysed per sample, unless noted otherwise.

Attenuated total reflection-Fourier transform infrared spectroscopy (ATR-FTIR) analysis was performed using a PerkinElmer Frontier (32 scans, scan range 4000-400 cm^{-1}, resolution 4 cm^{-1}).

Thermogravimetric analysis (TGA Q500, TA instruments, High-T Pt sample pan) was carried out from room temperature up to 900°C with a heating rate of 10°C/min in a dry air atmosphere (90 ml min^{-1}).

Dynamic light scattering (DLS) was performed with a Brookhaven ZetaPals. To this end dispersed CeO_{2-x} samples from hydrothermal synthesis were diluted with ultrapure water for measurement. Five measurements (two minutes each) were carried out per sample.

Raman spectra were collected using a Renishaw InVia Qontor Confocal Raman Microscope with a 100x objective and a 785 nm laser excitation source (100 mW). Calibration of the Raman shift scale was performed with Silicon. Measurements were performed at room temperature in air with a low laser power (0.05 %) to guarantee the sample to be unaffected during laser exposure. An exposure time of 30 seconds (60 summations) was performed using a 1200 l/mm grating. Processing of Raman spectra, background subtraction and cosmic ray removal, was carried out in the Renishaw WiRe software.

Powder X-ray diffraction was carried out using a Bruker D8 Discover (Cu K-α radiation, LynxEye detector). 100 mg of LaB_6 (Alfa Aesar, 99.5%) was added as an internal standard to 100 mg sample. Measurements were carried out from 2θ value of 10° to 130° with a step size of 0.01° and step time of 3 seconds. Le Bail refinement was carried out in the JANA2006 software to obtain cell parameters.[13]

UV-Visible diffuse reflectance spectrometry was performed with a Cary UV-Vis-NIR spectrometer, Agilent Technologies. The sample (500 mg) was added to the powder holder and reflectance was measured in scan mode with a scan rate of 10 nm/s, with a range between 300 nm and 800 nm. A sample holder containing PTFE was used to construct a baseline (100% reflectance) while a zero-reference point was constructed in absence of a sample holder (0% reflectance).

Brunauer-Emmett-Teller (BET) theory was applied on N_2 physisorption isotherms (Micromeritics, Tristar II, -196°C) of the photocatalysts in order to determine the specific surface area. Samples were

flushed with nitrogen gas at 150°C for 16h prior to the measurement in order to remove possible residual adsorbed components.

Au content in the Au/CeO_{2-x} photocatalysts was determined with inductively coupled plasma-optical emission spectrometry (ICP-OES), Perkin Elmer Optima 330 dv simultaneous spectrometer, PerkinElmer, Waltham, MA, USA. Sample digestion was carried out in a 10 ml mixture of mineral acids (HCl (≥37%, TraceSELECT, for trace analysis, Honeywell chemicals):HNO_3 (69.0-70.0%, J.T.Baker, for trace metal analysis):HF (40%, AnalaR NORMAPUR® analytical reagent, VWR) in a 3.17:1:1.71 ratio) in a Milestone microwave setup. For ICP-OES measurements, 1000 ppm Au standard (Merck) and the sample solutions were diluted by 5% HNO_3 to 1-2-5-10 ppm and 1-10 ppm concentrations, respectively. All ICP analyses were carried out *in duplo*.

Hydrogen-temperature programmed reduction (H_2-TPR) was performed with a Chemstar TPX Chemisorption Analyzer (Quantachrome). First the sample was degassed (typically 50 mg) at 300°C for 2h with 40 ml min^{-1} He flushing, after which the sample was cooled down to 50°C. H_2-TPR was performed from 50°C to 900°C at a heating rate of 10°C/min under 40 ml min^{-1} 5% H_2/Ar flow.

1.3 Photocatalytic experiments

The catalytic CO_2 conversion tests were carried out in a custom-made reactor, a quartz window at the top allows for light irradiation, as described by Sastre et al.[14] Light for photocatalysis was supplied by a solar simulator (Newport Sol3A) situated above the reactor and was equipped with a high flux beam concentrator (Newport 81,030), and AM1.5 filter. Intensity of the irradiated light was calibrated with a thermopile sensor. For experiments without UV component, an additional filter was mounted cutting off wavelengths below 395 nm. The irradiated area was about 3.14 cm^2, which was fully covered by the sample catalyst. Temperature during reaction was monitored by three thermocouples: top of the reactor, bottom of reactor, bottom of the catalyst bed. In addition, temperature inside the catalyst bed was monitored by four optical Fibre Bragg Gratings (FBG) as described by Xu et al.[15] at depths of 0 mm, 0.15 mm, 0.30 mm and 0.50 mm. A fifth FBG was placed on the rim of the catalyst holder as a reference. In a typical experiment, 200 mg of the catalyst was loaded in the catalyst holder and flattened homogeneously for accurate FBG measurements. The reactor was then vacuum purged and filled with N_2 in three cycles. Next, a constant flow of a mixture of H_2 (Linde 6.0), CO_2 (Linde 4.5) and N_2 (Linde 5.0), with flow rates of 8 ml min^{-1}, 8 ml min^{-1} and 4 ml min^{-1}, respectively, was allowed through the catalyst bed. A reactor pressure of 3.5 bar was maintained by a backpressure regulator. The lamp was switched on after 20 minutes of flow. In dark reaction conditions, the reactor vessel was heated to 180°C under vacuum, once the temperature stabilised the gas flow was initiated. The reaction products were analysed by a gas chromatograph (Compact GC, Global Analyzer Solutions), and injections were automatically taken every 2.5 min from the outgoing flow. The GC was equipped with three channels, two microthermal conductivity detectors (TCD) and one flame ionisation detector (FID). The peak areas were used to determine the ratio of all components based on calibration, N_2 being used as an internal standard. If any products were present in the time zero analysis, this value was subtracted from the following results.

Catalytic tests with varied catalyst loading were performed with a custom-made reactor, a quartz window at the top allows for light irradiation. Light for catalysis was supplied by a 300 W Xe Arc lamp (LOT-Quantum Design, LSB531). The irradiated area was about 2.14 cm^2, where the sample catalyst homogeneously covered the area. In a typical experiment, the catalyst was loaded in the reactor, the reactor was then vacuum purged and filled with a mixture of H_2 (Air Liquide, P0232), CO_2 (Air Liquide, P1209) and N_2 (Air Liquide, P0271) at constant flow rates of 8 ml min^{-1}, 8 ml min^{-1} and 4 ml min^{-1}, respectively. A reactor pressure of 3.5 bar was maintained by a backpressure regulator. The lamp was

switched on after 30 minutes of flow. The reaction products were analysed by a gas chromatograph (Agilent, 990 Micro GC) with two TCD channels (MS5A SS column for H_2, O_2, N_2, CH_4 and CO and PORAPLOT U column for CO_2 and C_2+ components). The peak areas were used to determine the ratio of all components based on calibration, N_2 being used as an internal standard. If any products were present in the time zero analysis, this value was subtracted from the following results.

Sample	**CeO_2 size /nm**	**Au size /nm**	**Au loading /wt. %**	**Thermal treatment**
L-HT	200 ± 7	/	/	/
L	196 ± 13	/	/	400°C (Dry Air)
4Au/L	/	3.5 ± 0.2	4.0 ± 0.8	/
4Au/L-O	/	5.1 ± 0.3	4.0 ± 0.8	500°C (Dry Air)
4Au/L-R	/	3.0 ± 0.3	4.0 ± 0.8	500°C (5% H_2)
S-HT	35.5 ± 0.7	/	/	/
S	37 ± 2	/	/	400°C (Dry Air)
4Au/S	/	3.6 ± 0.3	3.8 ± 0.9	/
4Au/S-O	/	4.9 ± 0.4	3.8 ± 0.9	500°C (Dry Air)
4Au/S-R	/	3.8 ± 0.4	3.8 ± 0.9	500°C (5% H_2)
0.4Au/S	/	<2	0.41 ± 0.02	/
1.5Au/S	/	3.9 ± 0.3	1.57 ± 0.08	/
6Au/S	/	3.5 ± 0.3	5.8 ± 0.4	/

Table S2: Summary of synthesised samples and their characterisation, 98% confidence intervals are reported

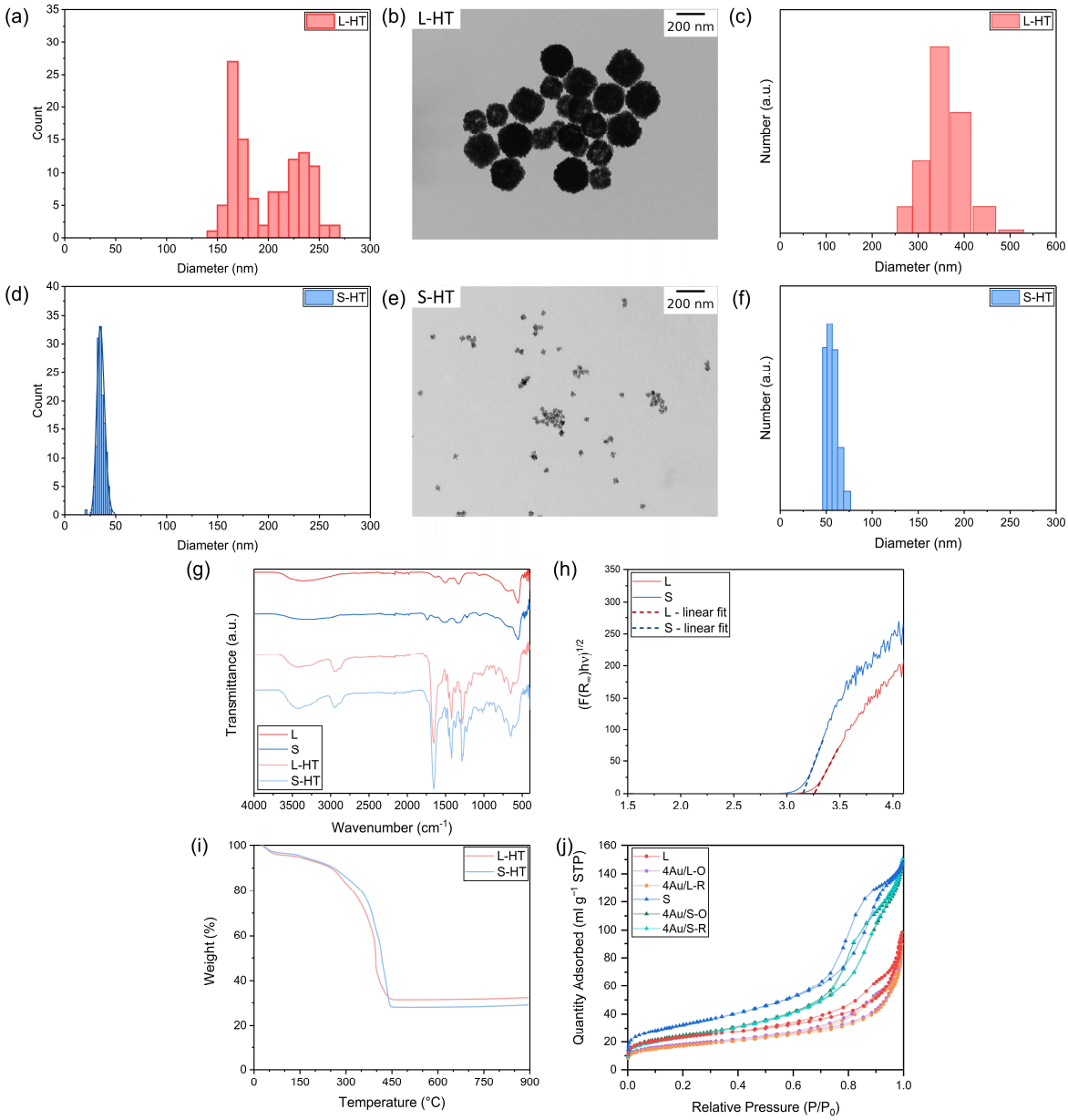

Fig. S1: (a) Particle size distribution of L-HT CeO_2 support from TEM analysis; (b) representative TEM image of L-HT CeO_2 particles; (c) particle size distributions of L-HT CeO_2 sample from DLS; (d) particle size distribution of S-HT CeO_2 support from TEM analysis with lognormal fit; (e) representative TEM image of S-HT CeO_2 particles; (f) particle size distributions of L-HT CeO_2 sample from DLS; (g) ATR-FTIR spectrograms of L, S L-HT and S-HT CeO_2 particles, graphs have been stacked for visual clarity; (h) Tauc analysis of diffuse reflectance UV-Vis measurements of L and S CeO_2 particles, band gap energy is determined by intercept of the linear fit with the x-axis; (i) TGA analysis of L-HT and S-HT samples; (j) N_2 adsorption isotherms of L, 4Au/L-O, 4Au/L-R, S, 4Au/S-O and 4Au/S-R samples.

L		S	
Wavenumber /cm^{-1}	**Origin**	**Wavenumber /cm^{-1}**	**Origin**
>3000	H_2O	>3000	H_2O
		1741, 1727	Bridged carbonate
1640	H_2O	1636	H_2O
1500	Bidentate carbonate	1506	Bidentate carbonate
1330	Unidentate carbonate	1473, 1352	Unidentate carbonate
		1230, 1217	Bridged carbonate
1063, 845	Unidentate carbonate	1057, 843	Unidentate carbonate
686, 590, 550	CeO_2	674, 583, 552	CeO_2

Table S3: Assignment of main peaks found in the ATR-FTIR of L and S following Li et al. [16].

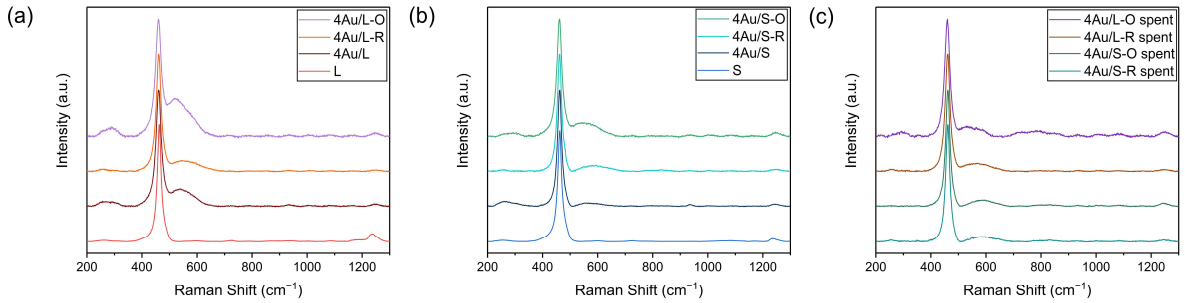

Fig. S2: Raman spectra of (a) 4Au/L-O, 4Au/L-R, 4Au/L, and L, (b) 4Au/S-O, 4Au/S-R, 4Au/S and S, (c) 4Au/L-O spent catalyst, 4Au/L-R spent catalyst, 4Au/S-O spent catalyst and 4Au/S-R spent catalyst. Intensity has been normalised on the intensity of the F_{2g} peak, graphs have been stacked for visual clarity.

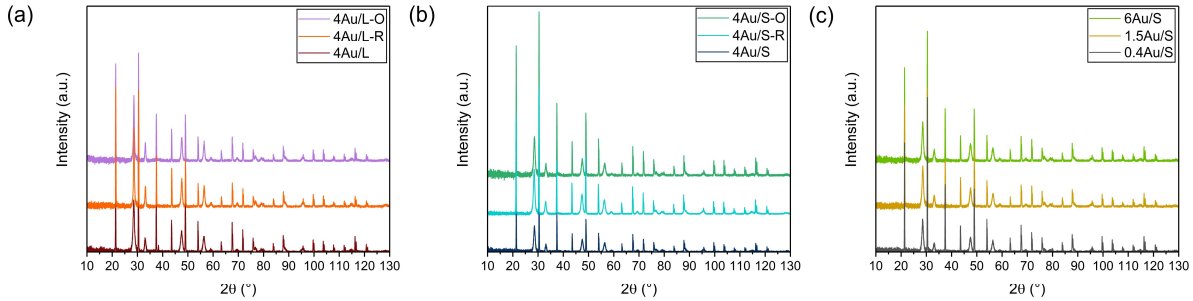

Fig. S3: XRD diffractograms of (a) 4Au/L-O, 4Au/L-R and 4Au/L, (b) 4Au/S-O, 4Au/S-R and 4Au/S, (c) 6Au/S, 1.5Au/S and 0.4Au/S with LaB_6 as internal standard, intensity is normalised on the wt% of sample in the sample/LaB_6 mixture, graphs have been stacked for visual clarity.

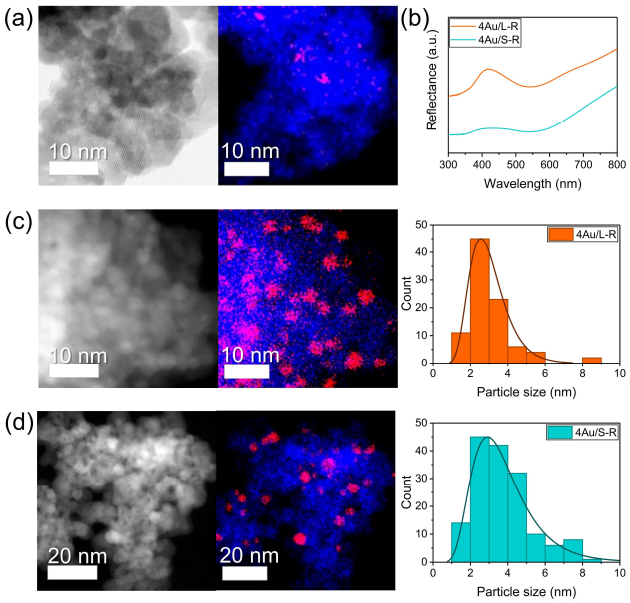

Fig. S4: (a) Representative annular bright field-STEM image and EDX mapping in STEM mode of 0.4Au/S, CeO_2 is coloured blue and Au is coloured red in the EDX mapping; (b) diffuse reflective UV-Vis spectra of 4Au/L-R and 4Au/S-R, graphs have been stacked for visual clarity; Representative HAADF-STEM image, EDX mapping in STEM mode and Au particle size distribution from TEM analysis with lognormal fit of (c) 4Au/L-R and (d) 4Au/S-R, CeO_2 is coloured blue and Au is coloured red in the EDX mapping.

Sample	TPR: %H_2 uptake CeO_{2-x} surface
L	41.8
4Au/L	18.7
4Au/L-O	25.7
4Au/L-O spent	16.7
4Au/L-R	16.0
4Au/L-R spent	18.2
S	55.2
4Au/S	31.7
4Au/S-O	30.6
4Au/S-O spent	24.3
4Au/S-R	20.6
4Au/S-R spent	22.5

Table S4: %H_2 uptake at the surface of CeO_{2-x} normalised on the total H_2 uptake in the sample in H_2-TPR. H_2 uptake peaks under 500°C are considered originating from the CeO_{2-x} surface.

	9 kW m^{-2} illumination and no external heating			**No illumination and external heating to 180°C**		
Sample	**CO production /mmol g_{Au}^{-1} h^{-1}**	**CH_4 production /mmol g_{Au}^{-1} h^{-1}**	**CO selectivity /%**	**CO production /mmol g_{cat}^{-1} h^{-1}**	**CH_4 production /mmol g_{cat}^{-1} h^{-1}**	**CH_4 selectivity /%**
L	0	0	/	0	2.22 ± 0.02	100
4Au/L-O	1.06 ± 0.09	0.0014 ± 0.0005	99.8	0.017 ± 0.005	2.156 ± 0.003	99.2
4Au/L-R	2.2 ± 0.2	0.0025 ± 0.0006	99.9	0.061 ± 0.006	1.990 ± 0.003	97.0
S	0	0	/	0	2.620 ± 0.004	100
4Au/S-O	1.4 ± 0.4	0.0054 ± 0.0009	99.6	0.010 ± 0.002	1.767 ± 0.003	97.8
4Au/S-R	2.8 ± 0.2	0.039 ± 0.002	98.6	0.032 ± 0.005	1.435 ± 0.002	97.8
0.4Au/S	3.9 ± 0.7	0.08 ± 0.02	99.4	/	/	/
1.5Au/S	1.0 ± 0.1	0.017 ± 0.003	98.3	/	/	/
6Au/S	1.8 ± 0.2	0.0054 ± 0.0004	99.7	/	/	/

Table S5: Summary of catalysis results, confidence intervals of 98% are shown.

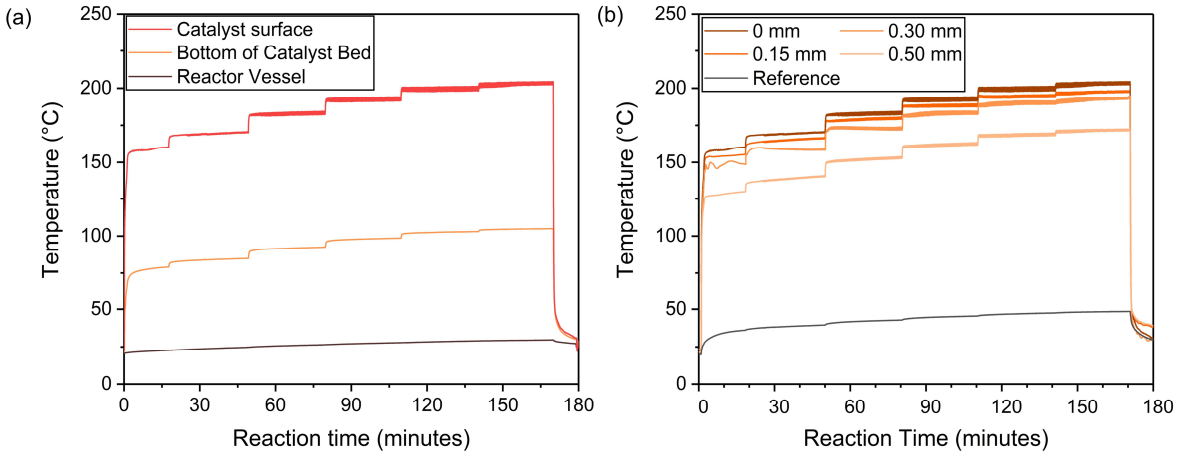

Fig. S5: (a) Temperature of reactor vessel, bottom of the catalyst bed and top of the catalyst of 4Au/S-R light variation experiments. (b) Temperature gradient inside the catalyst bed determined by FBGs at the catalyst surface, 0.15 mm depth, 0.30 mm depth and 0.50 mm depth during 4Au/S-R light variation experiment. Additionally, a reference FBG was present on the catalyst holder.

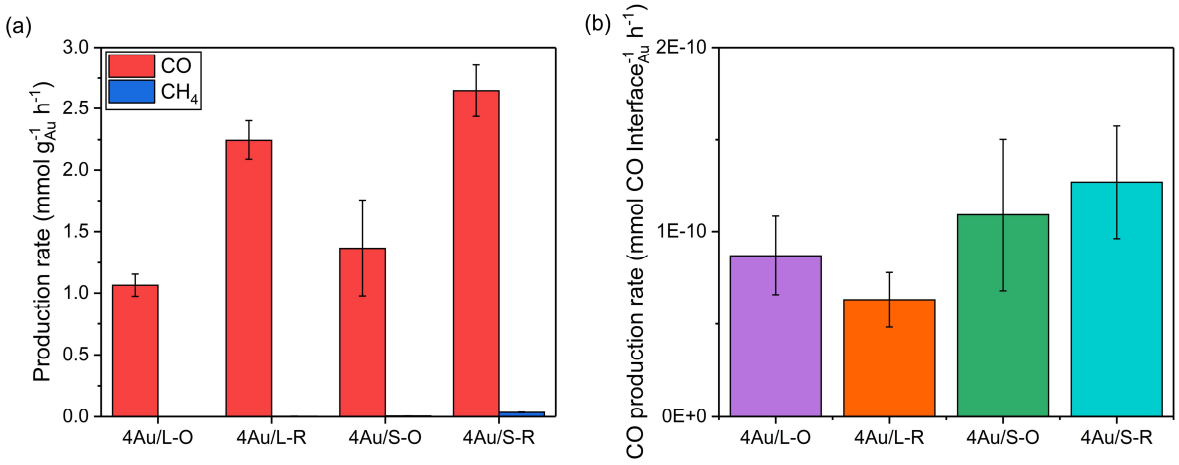

Fig. S6: (a) CO and CH_4 production rates of 4Au/L-R, 4Au/L-O, 4Au/S-R and 4Au/S-O under illumination (b) CO production rates of 4Au/L-R, 4Au/L-O, 4Au/S-R and 4Au/S-O under illumination normalised on circumference of Au particles. Reaction conditions: mixture of CO_2:H_2:N_2 (8 ml min^{-1} :8 ml min^{-1}:4 ml min^{-1}) at 3.5 bar pressure, 200 mg Au/CeO_2 photocatalyst, 9 kW m^{-2} illumination from solar simulator (AM1.5).

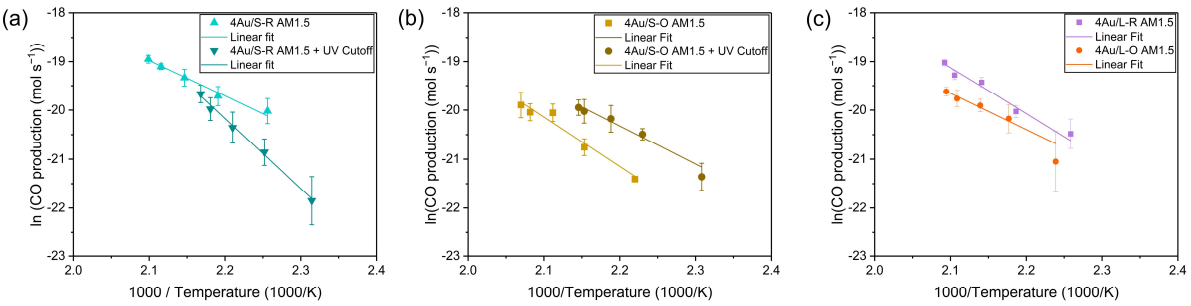

Fig. S7: Arrhenius plots of (a) 4Au/S-R and (b) Au/S-O under varied illumination using AM1.5 filter and AM1.5 + UV cutoff filter and (c) 4Au/L-R and 4Au/L-O under varied illumination using AM1.5 filter. Confidence intervals of 98% are reported.

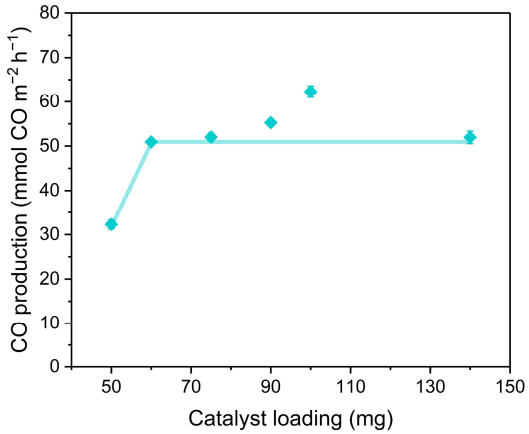

Fig. S8: CO production normalised on illuminated area in function of catalyst loading of 4Au/S-R. Confidence intervals of 98% are reported. Reaction conditions: mixture of CO_2:H_2:N_2 (8 ml min^{-1} :8 ml min^{-1}:4 ml min^{-1}) at 3.5 bar pressure, varied loading of Au/CeO_2 photocatalyst, 8.4 kW m^{-2} illumination from 300W Xe Arc lamp.

Sample	CO production		
	/mmol g_{Au}^{-1} h^{-1}	/10^{-11} mmol C_{Au}^{-1} h^{-1}	/10^{-19} mmol #$particles_{Au}^{-1}$ h^{-1}
0.4Au/S	3.9 ± 0.7	1.8 ± 0.7	1.0 ± 0.5
1.5Au/S	1.0 ± 0.1	2.3 ± 0.4	2.9 ± 0.7
6Au/S	1.8 ± 0.2	3.5 ± 0.7	4 ± 1

Table S6: Summary of calculated values in order to correlate CO production rate to Au size and loading. C is the circumference of the circle at the interface between metal and support. The size of Au in 0.4Au/S was assumed to be 1.7 ± 0.3 nm for the calculations. Confidence intervals of 98% are reported on these values.

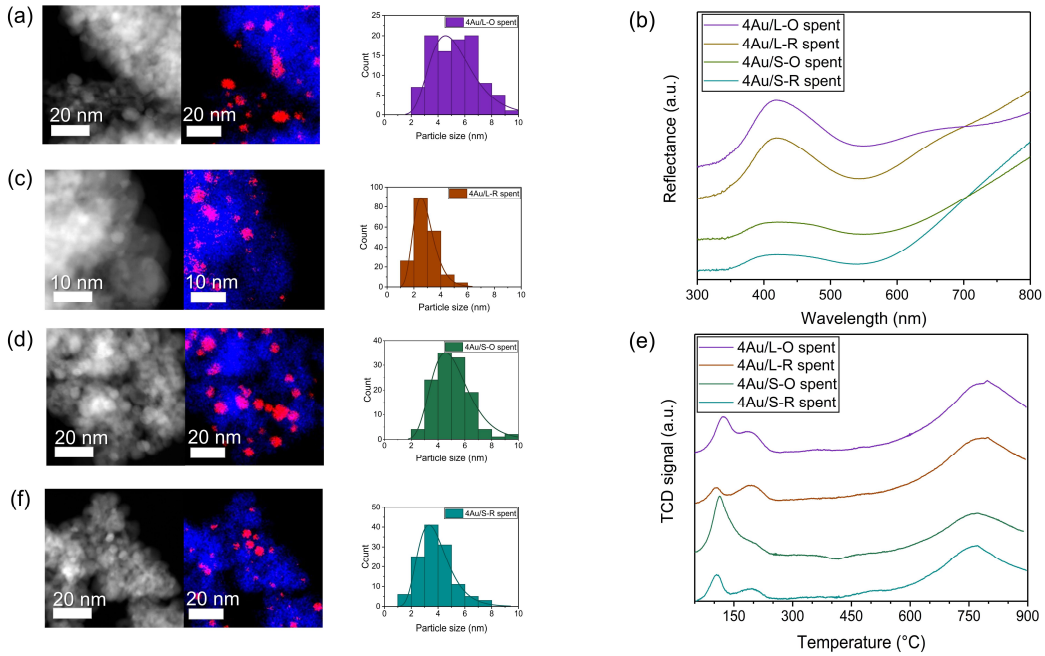

Fig. S9: Representative HAADF-STEM image, EDX mapping in STEM mode and Au particle size distribution from TEM analysis with lognormal fit of (a) 4Au/L-O spent catalyst, (c) 4Au/L-R spent catalyst, (d) 4Au/S-O spent catalyst and (f) 4Au/S-R spent catalyst, CeO_2 is coloured blue and Au is coloured red in EDX mapping; (b) reflective diffuse UV-Vis spectra of 4Au/L-O, 4Au/L-R, 4Au/S-O and 4Au/S-R spent catalysts, graphs have been stacked for visual clarity; (e) H_2-TPR profiles of 4Au/L-O, 4Au/L-R, 4Au/S-O and 4Au/S-R spent catalysts, graphs have been stacked for visual clarity.

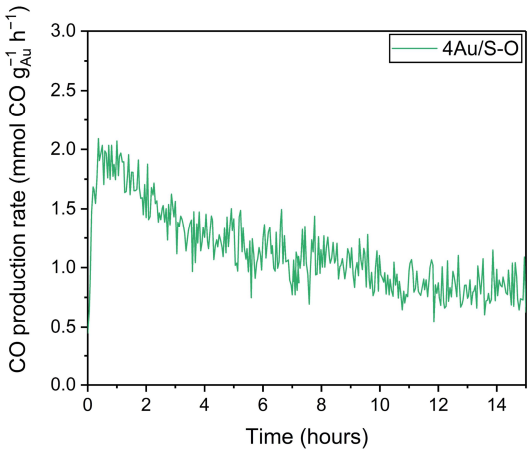

Fig.S10 CO production of 4Au/S-O over 15h. Reaction conditions: mixture of CO_2:H_2:N_2 (8 ml min^{-1} :8 ml min^{-1}:4 ml min^{-1}) at 3.5 bar pressure, 200 mg Au/CeO_2 photocatalyst, 9 kW m^{-2} illumination from solar simulator (AM1.5).

2 References:

1. A. A. Upadhye, I. Ro, X. Zeng, H. J. Kim, I. Tejedor, M. A. Anderson, J. A. Dumesic and G. W. Huber, Plasmon-enhanced reverse water gas shift reaction over oxide supported Au catalysts, *Catalysis Science & Technology*, 2015, **5**, 2590-2601.
2. B. Tahir, M. Tahir and N. A. S. Amin, Photocatalytic CO_2 conversion over Au/TiO_2 nanostructures for dynamic production of clean fuels in a monolith photoreactor, *Clean Technologies and Environmental Policy*, 2016, **18**, 2147-2160.
3. P. Martínez Molina, N. Meulendijks, M. Xu, M. A. Verheijen, T. den Hartog, P. Buskens and F. Sastre, Low Temperature Sunlight-Powered Reduction of CO_2 to CO Using a Plasmonic Au/TiO_2 Nanocatalyst, *ChemCatChem*, 2021, **13**, 4507-4513.
4. P. Martínez Molina, K. W. Bossers, J. D. Wienk, J. Rohlfs, N. Meulendijks, M. A. Verheijen, P. Buskens and F. Sastre, Sunlight Powered Continuous Flow Reverse Water Gas Shift Process Using a Plasmonic Au/TiO_2 Nanocatalyst, *Chemistry – An Asian Journal*, 2023, **18**, e202300405.
5. J. Volders, K. Elen, A. Raes, R. Ninakanti, A.-S. Kelchtermans, F. Sastre, A. Hardy, P. Cool, S. W. Verbruggen, P. Buskens and M. K. Van Bael, Sunlight-Powered Reverse Water Gas Shift Reaction Catalysed by Plasmonic Au/TiO_2 Nanocatalysts: Effects of Au Particle Size on the Activity and Selectivity, *Nanomaterials*, 2022, **12**, 4153.
6. X. Zhang, X. Li, D. Zhang, N. Q. Su, W. Yang, H. O. Everitt and J. Liu, Product selectivity in plasmonic photocatalysis for carbon dioxide hydrogenation, *Nature Communications*, 2017, **8**, 14542.
7. K. Wang, S. Shao, Y. Liu, M. Cao, J. Yu, C. H. Lau, Y. Zheng and X. Fan, DRIFTS-SSITKA-MS investigations on the mechanism of plasmon preferentially enhanced CO_2 hydrogenation over Au/γ-Al_2O_3, *Applied Catalysis B: Environmental*, 2023, **328**, 122531.
8. I. Ro, R. Carrasquillo-Flores, J. A. Dumesic and G. W. Huber, Intrinsic kinetics of plasmon-enhanced reverse water gas shift on Au and Au–Mo interfacial sites supported on silica, *Applied Catalysis A: General*, 2016, **521**, 182-189.
9. B. Lu, F. Quan, Z. Sun, F. Jia and L. Zhang, Photothermal reverse-water-gas-shift over Au/CeO_2 with high yield and selectivity in CO_2 conversion, *Catalysis Communications*, 2019, **129**, 105724.
10. Q. Wang, W. Jia, B. Liu, W. Zhao, C. Li, J. Zhang and G. Xu, Controllable Synthesis of Nearly Monodisperse Spherical Aggregates of CeO_2 Nanocrystals and Their Catalytic Activity for HCHO Oxidation, *Chemistry – An Asian Journal*, 2012, **7**, 2258-2267.
11. R. Zanella, S. Giorgio, C. R. Henry and C. Louis, Alternative Methods for the Preparation of Gold Nanoparticles Supported on TiO_2, *The Journal of Physical Chemistry B*, 2002, **106**, 7634-7642.
12. J. Matos, T. Marino, R. Molinari and H. García, Hydrogen photoproduction under visible irradiation of Au–TiO_2/activated carbon, *Applied Catalysis A: General*, 2012, **417-418**, 263-272.
13. V. Petříček, M. Dušek and L. Palatinus, Crystallographic Computing System JANA2006: General features, *Zeitschrift für Kristallographie - Crystalline Materials*, 2014, **229**, 345-352.
14. F. Sastre, C. Versluis, N. Meulendijks, J. Rodríguez-Fernández, J. Sweelssen, K. Elen, M. K. Van Bael, T. den Hartog, M. A. Verheijen and P. Buskens, Sunlight-Fueled, Low-Temperature Ru-Catalyzed Conversion of CO_2 and H_2 to CH_4 with a High Photon-to-Methane Efficiency.*Journal*, 2019, **4**, 7369-7377.
15. M. Xu, T. den Hartog, L. Cheng, M. Wolfs, R. Habets, J. Rohlfs, J. van den Ham, N. Meulendijks, F. Sastre and P. Buskens, Using Fiber Bragg Grating Sensors to Quantify Temperature Non-Uniformities in Plasmonic Catalyst Beds under Illumination, *ChemPhotoChem*, 2022, **6**, e202100289.

16. C. Li, Y. Sakata, T. Arai, K. Domen, K.-i. Maruya and T. Onishi, Carbon monoxide and carbon dioxide adsorption on cerium oxide studied by Fourier-transform infrared spectroscopy. Part 1.—Formation of carbonate species on dehydroxylated CeO_2, at room temperature, *Journal of the Chemical Society, Faraday Transactions 1: Physical Chemistry in Condensed Phases*, 1989, **85**, 929-943.